PROC. 15TH INT. CONF. PHYSICS OF SEMICONDUCTORS, KYOTO, 1980
J. PHYS. SOC. JAPAN **49** (1980) SUPPL. A p. 215–222

THE ROLE OF THE LATTICE IN DEEP LEVELS AND NONRADIATIVE RECOMBINATIONS

D. V. Lang

Bell Laboratories
Murray Hill, New Jersey 07974

A review of nonradiative recombination and extrinsic self-trapping centers in III-V compounds is given, with particular emphasis on the role of the lattice phonons. We find that the data support the theoretical expectation that zone-edge TA phonons are the dominant distortion modes of extrinsic self-trapping and vacancy-like defects. Recent evidence supporting the microscopic model of DX centers is also discussed.

I. Introduction

The importance of localized lattice relaxation in determining the electronic properties of defects in ionic solids has long been recognized. On the other hand, except for the spin resonance studies of vacancies in Si by Watkins and Corbett [1], it was generally believed that such effects were unimportant in covalent semiconductors. However, since the work of Kukimoto and Henry [2] on oxygen in GaP there has been considerable evidence that lattice relaxation plays an important role in III-V semiconductors. The observation of recombination-enhanced defect motion in GaAs gave convincing support to the idea that strong lattice relaxations occurred during nonradiative recombination [3]. This was put on a more sound theoretical footing by the success of the nonadiabatic multiphonon emission model in explaining carrier capture at defects in GaAs and GaP [4]. Defects have recently been observed [5] in III-V mixed crystals which exhibit such a strong coupling to the lattice that the phenomenon of extrinsic self-trapping occurs [6]. Thus, there seems little doubt that strong electron-lattice coupling at deep level defects in covalent semiconductors can be as important as it is in ionic crystals.

In this paper we will examine the overall trends in the carrier capture rates at various deep levels in order to show explicitly the role of the lattice in nonradiative recombination. The major point which we find is the crucial role of specific types of host lattice phonons in determining the capture rate at low temperatures. In particular, the extrinsic self-trapping DX center in $Al_xGa_{1-x}As$ appears to couple strongly to short wavelength transverse acoustic (TA) phonons at the edge of the Brillouin zone. This is to be contrasted with nearly all other known defects or impurities (both shallow and deep) which couple predominantly to optic (TO or LO) phonons.

II. MPE Capture in the Strong-Coupling Regime

In general, we may express [4,7] the MPE capture cross section σ as

$$\sigma = Af(0) \ , \tag{1}$$

where A is a term involving only the electronic matrix elements of the transition and $f(h\nu)$ is the well-known optical lineshape for phonon-assisted absorption or emission transitions. The lineshape function $f(h\nu)$ has been evaluated in closed form for arbitrary coupling strength and temperature by Huang and Rhys [8], Kubo and Toyozawa [9], and Lax [10]. It is this function evaluated at $h\nu = 0$ which dominates the temperature dependence of the MPE capture rate. The contribution of Henry and Lang [4,11] to this problem was an attempt to approximately calculate the electronic term A for free-to-bound transitions between the continuum and bound states, respectively, of a spherical square well potential whose radius was modulated by the lattice. Their results were in surprisingly good agreement with experimental data for deep levels in GaAs and GaP.

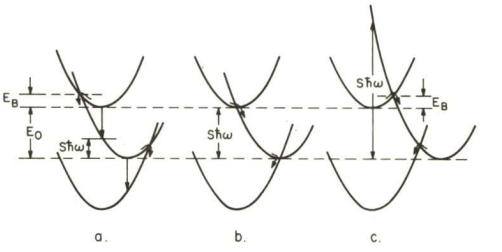

Figure 1. Configuration coordinate (cc) diagrams for progressively larger amounts of lattice relaxation energy, E_R. In all three cases the lowest curve corresponds to the total energy of the system in its ground state; the upper curve is the threshold energy of an e.h pair plus an empty defect; the shifted central curve is for a free h plus an occupied defect. (a) "normal" defect; (b) extrinsic self trapping with no barrier; (c) extrinsic self trapping with same barrier as in (a)

For the purpose of discussing the temperature dependence of MPE capture it is most instructive to focus attention on f(0) and to treat A as an adjustable parameter which may vary within approximately an order of magnitude of the Henry and Lang result ($A_{HL}=1.5\times10^{-14}cm^2eV$ for a neutral center [4]). In the limit of strong electron-phonon coupling $f(h\nu)$ approaches a Gaussian lineshape [7,10] and f(0) may be written [7] as

$$f(0) = (4\pi E_R kT^*)^{-1/2}\exp(-E_B/kT^*) \quad (2)$$

where $E_R = S\hbar\omega$ is the lowering of the energy of the bound state due to lattice relaxation, $\hbar\omega$ is the average energy of the phonons to which the defect is coupled, and E_B is the classical barrier height at the crossing of the configuration coordinate curves as shown in Fig. (1). The effective temperature T^* is defined as

$$kT^* = \frac{\hbar\omega}{2}\coth\left(\frac{\hbar\omega}{2kT}\right). \quad (3)$$

Thus at high temperatures $T^* = T$ and Eq. (2) shows the classical thermally activated capture first predicted by Mott [12]. At low temperatures $kT^* = \hbar\omega/2$ and the zero-point vibrations of the lattice play the role of temperature in promoting MPE transitions. Thus at low temperatures the log of the capture cross section is proportional to the number of phonons necessary to reach the classical barrier E_B. This behavior is reminiscent of the so-called "energy-gap law" characteristic of the low-temperature weak-coupling regime where the log of the capture rate is proportional to the number of phonons needed to equal to the *depth* of the level E_0 [7,13]. It has been recently proposed [13] that this weak-coupling "energy-gap law," which is valid for large molecules [7] and for narrow-line emissions in solids [14,15], ought to also roughly describe the low temperature behavior of even more strongly coupled defects. As we shall see, such an expectation is not supported by the deep-level capture data in GaAs and GaP [4].

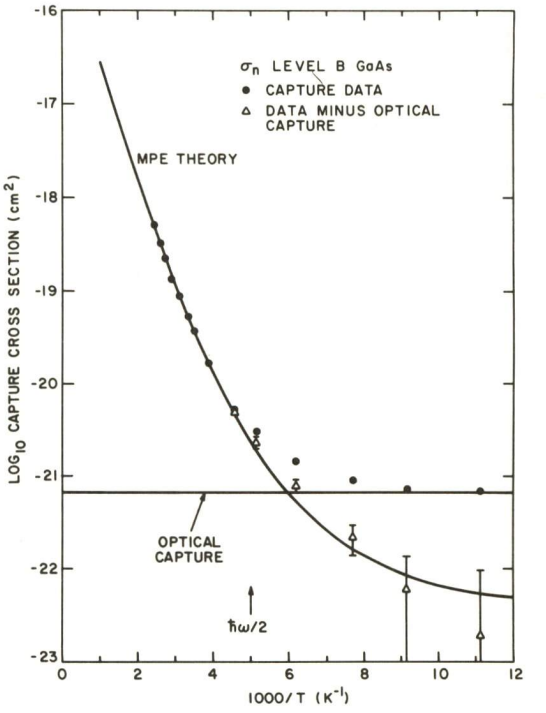

Figure 2. Fit of the strong-coupling MPE expression to the electron apture cross section for level B in GaAs: Adjustable parameters are A, E_B, and σ_{op}. ($\hbar\omega$ is set at 34 meV)

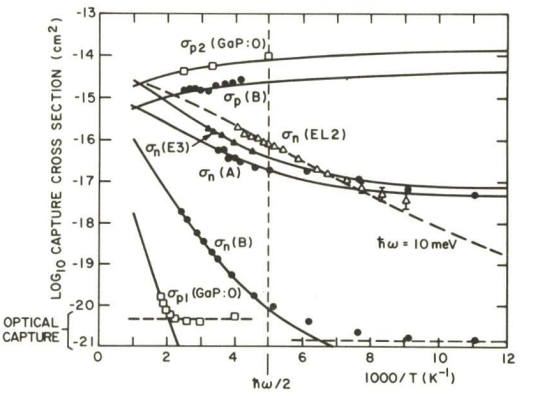

Figure 3. Fit of the strong-coupling MPE expression to a range of typical capture cross sections for deep levels in GaAs and GaP: The specific values of the fitting parameters are less important tha the fact that the overall trends of the data are easily accounted for by this expression

The coupling strength parameter G is approximately given by [7]

$$G = S \coth\left(\frac{\hbar\omega}{2kT}\right) \quad , \tag{4}$$

where $S = E_R/\hbar\omega$ is often called the Huang-Rhys factor [8]. The strong-coupling regime is then defined [7] as $G >> 1$; the weak-coupling case corresponds to $G \leq 1$. However, in spite of the fact that these two regimes are well-defined mathematically, it is often difficult to determine which is more appropriate to a particular set of experiment data. A case in point is the so-called level B in GaAs [16]. The electron capture data [4,16,17] for this level have been fit by various MPE expressions with three widely different values of S, namely, $S = 0.5 - 1$ [18], $S = 3.0$ [20], and $S = 7.7$ [19]. These values range from the weak ($S \leq 1$) to strong ($S >> 1$) coupling regimes. In Fig. (2) we show our own fit to the level-B data [21] using Eqs. (1)-(3) with $A = 0.07A_{HL}$, $S = 5.9$, and $\hbar\omega = 34$ meV. Since $E_0 = 0.72$ eV in this case, the classical barrier height in Fig. (2) is $E_B = 0.33$ eV. This is to be compared with the apparent asymptotic slope of the data of 0.25 eV. About half of this difference (kT=0.04 eV at 500K) can be accounted for by the T^{-1} behavior of the exponential prefactor, with the balance due to the fact that the system is not totally in the high temperature limit even for the highest temperature data.

The sharp transition at about $1000/T = 6$ between nearly temperature independent and nearly activated behavior in Fig. (2) is far too abrupt to be fit by MPE capture. Therefore, as has been suggested by Burt [20], another capture mechanism must be operative. Since Henry and Lang [4] clearly ruled out Auger capture for this particular case, and since the center is most likely neutral before electron capture, the only possible mechanism is optical capture by emission of a photon. It is possible to estimate the effective cross section σ_{op} for optical capture from experimental values for the photoionization cross section $\sigma^0(E)$ as measured by junction photocurrent or photocapacitance. From the well-known Einstein relations between absorption and spontaneous emission [22] we have for the case of electron capture

$$\sigma_{op} = 3.5\times10^{19}\left[\frac{\bar{n}^2E^2T}{vN_c}\right]\sigma_n^0(E) \quad , \tag{5}$$

where $\bar{n}$ is the refractive index, E the photon energy (eV) at the threshold of $\sigma^0(E)$, v is the thermal velocity (cm/s) of free carriers and $N_{c(v)}$ is the effective-mass density of states in the conduction (valence) band (cm^{-3}). For typical values [23] of σ^0 within kT of threshold ($10^{-17} \lesssim \sigma^0 \lesssim 10^{-16}$ cm^2) we have $10^{-21} \lesssim \sigma_{op} \lesssim 10^{-20}$ cm^2. The optical capture cross section needed to fit the data in Fig. (2) is in this approximate order of magnitude range.

Figure (3) shows the capture data from ref. 4 where the solid lines are calculated using Eqs. (1)-(3) with $\hbar\omega = 34$ meV and with $0.03 \lesssim A/A_{HL} \lesssim 1$ and $0 < E_B < 0.6$ eV treated as adjustable parameters. It is clearly possible to fit the general trends of the data with the strong coupling result of Eq. (2). Note in particular that the low temperature data are totally unrelated to the depths of the traps and hence cannot possibly be described by the weak-coupling "energy-gap law." For example σ_{p1} and σ_{p2} for GaP:0 differ by more than six orders of magnitude yet both correspond to $E_0 \sim 1.3$ eV. Similarly $\sigma_n(A) >> \sigma_n(B)$, while $E_0 = 1.0$ eV for level A and $E_0 = 0.72$ eV for level B. Indeed, it is one of the major triumphs of the strong-coupling MPE theory that $\sigma_{p2} = 10^{-14}$ cm^2 for GaP:0 can be fit by the theory in spite of the fact that this is one of the deepest states ($\sim$1.3 eV) studied.

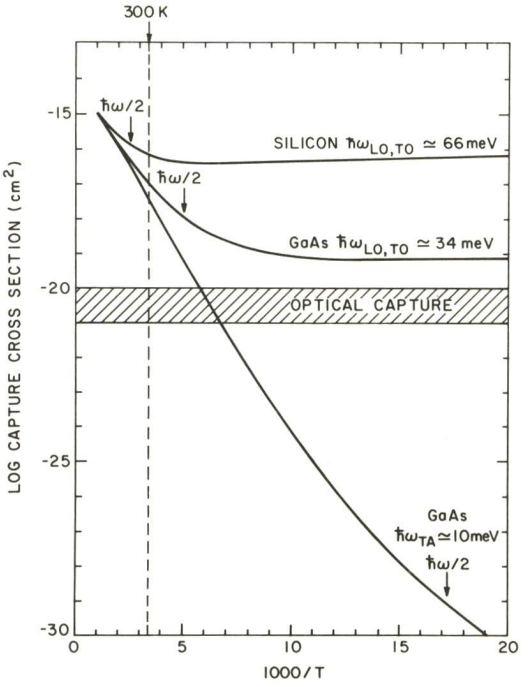

Figure 4. Equations (1)-(3) plotted for various phonon energies

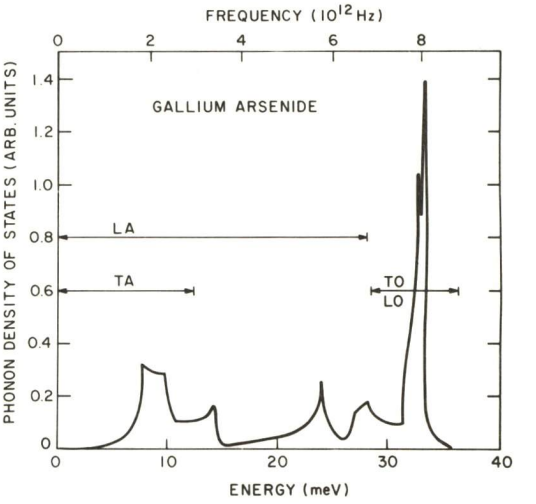

Figure 5. Phonon density of states in GaAs (after Dolling and Cowley [25]).

III. The Crucial Role of the Phonon Energy in Low Temperature Capture

From Eq. (3) it is evident that the average energy of the phonons coupling most strongly to the defect is the determining factor in separating the high and low temperature regimes. The midpoint of the transitional temperature range is at $kT = \hbar\omega/2$. In Fig. (3) this corresponds to T = 200K for $\hbar\omega$ = 34 meV. Note, however, that the capture cross section of the EL2 trap (formally called "0") [24] does not have a "knee" at 200K but is thermally activated to much lower temperatures. This fact has be cited as evidence that the activation barrier for this trap is electronic in origin rather than due to MPE [18]. Note, however, that the EL2 data in Fig. (3) can be fit quite well by Eqs. (1)-(3) with a phonon energy of 10 meV. The very strong dependence on phonon energy is best illustrated in Fig. (4) where we show theoretical curves for three different phonon energies all with $E_B = 0.25$ eV. The phonon energies of 10 and 34 meV were specifically chosen to match the regions of maximum density of states in the phonon spectrum of GaAs as shown in Fig. (5) [25]. Defects which couple to the LO or TO phonons would tend to have $\hbar\omega$ = 34 meV while those which couple to TA phonons would have $\hbar\omega$ = 10 meV. The phonon spectrum of silicon [25] has the same shape as that in Fig. (5) except that the energy scale is a factor of two larger for Si. Thus defects in silicon which couple to optical phonons would tend to have rather large, very weakly temperature dependent cross sections below 300K in agreement with the experimental results [26].

IV. Extrinsic Self Trapping: DX Centers in $Al_xGa_{1-x}As$

A very striking example of large electron-lattice coupling in III-V semiconductors is the case of the so-called DX centers in $Al_xGa_{1-x}As$ [5,27-29] and $GaAs_{1-x}P_x$ [30]. The type of cc diagram which describes this class of traps is shown in Fig. (1b,c) and in Fig. (6). The characteristic feature of these traps is that the lattice relaxation energy $E_R = S\hbar\omega$ is equal to or larger than the net equilibrium trap depth E_0. This is an example of the phenomenon which Toyozawa has called extrinsic self trapping [6,31]. In such a case the unrelaxed defect potential does not produce a bound state in the gap when the defect is unoccupied. However, the combined effect of both the electron-lattice coupling and the defect potential produces a bound state when the defect is occupied. Thus the presence of the electron at the defect *creates* the trap level, i.e., the carrier is self trapped at the defect. In more ionic materials such phenomenon can occur intrinsically at every lattice site without a defect potential. The resulting self-trapped carrier is often referred to as a "small" or acoustic polaron [6,31,32].

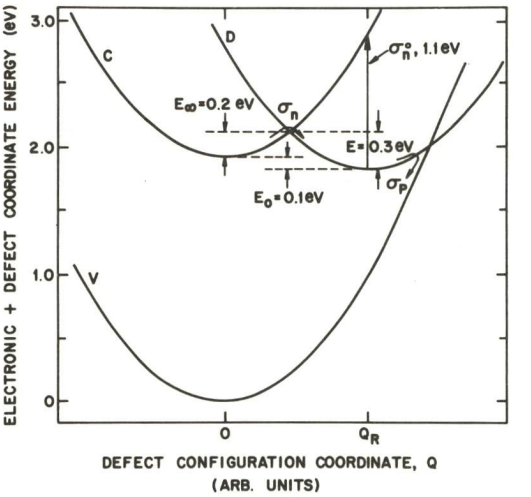

Figure 6. Semiquantitative configuration coordinate diagram for DX center in Te-doped $Al_xGa_{1-x}As$ (after Lang and Logan [27])

The original cc diagram shown in Fig. (6) was proposed [27] to semiquantitatively explain the properties of DX centers in Te-doped $Al_xGa_{1-x}As$ and thereby to explain the persistent photo-induced conductivity effect seen in that material [28]. More quantitative fits to the optical [5] and capture [27] data using the strong-coupling MPE limit for $f(h\nu)$ and $f(0)$, respectively, are shown in Figs. (7) and (8). The shape and temperature shift of the optical electron emission cross section was best fit with $E_R = 0.75 \pm 0.1$ eV, $E_0 = 0.10 \pm 0.05$ eV, and $\hbar\omega = 10$ meV [5]. We have fit the temperature dependence of the capture rate (σvn) data in ref. 27 using Eqs. (1)-(3) for $\sigma(T)$ in Fig. (8) [33]. The best fit is for $E_B = 0.32$ eV and $\hbar\omega = 10$ meV.

Just as we saw in Fig. (4), the fits in Figs. (7) and (8) are extremely sensitive to the value used for $\hbar\omega$, with the theory diverging strongly from the data for $\hbar\omega$ outside of the range 5-15 meV. From the phonon spectrum in Fig. (5) this is very strong evidence that the dominant phonons responsible for the large relaxation of the DX center are zone-edge TA phonons. Indeed, it is the 10 meV TA phonon frequency along with the impossibility of optical capture of an electron in Fig. (6) which actually accounts for the persistent photoconductivity effect [27,28].

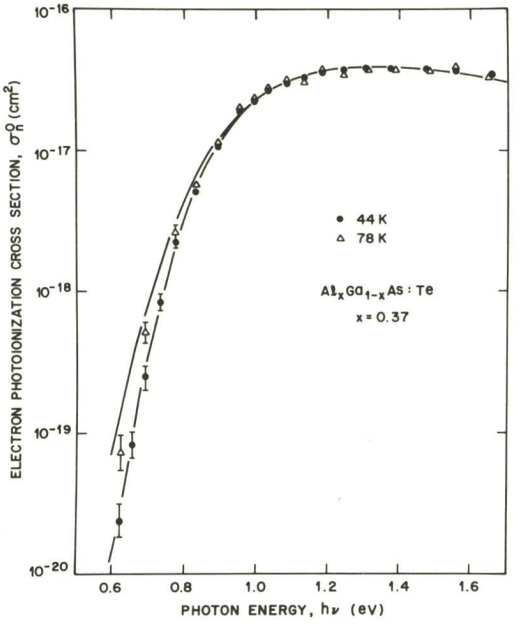

Figure 7. MPE fit to optical cross section for electron emission from DX center in $Al_xGa_{1-x}As$:Te. (after Lang et al [5]).

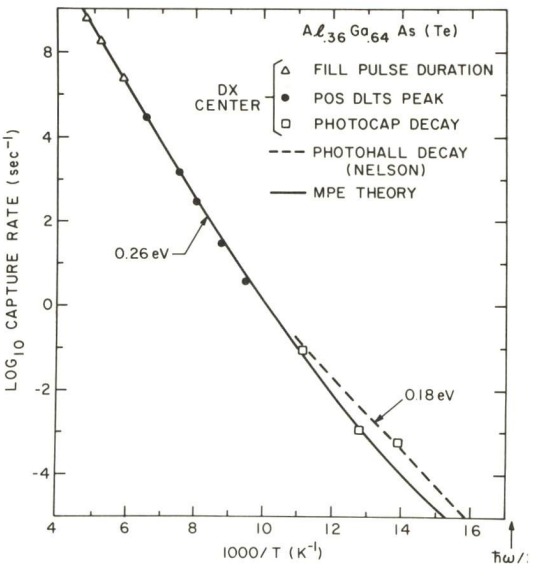

Figure 8. MPE fit to electron capture rate at DX centers in $Al_xGa_{1-x}As$:Te (data from refs 27, 28)

The dominant role of TA phonons for certain defects is exactly what one should have expected from defect theories, although little attention has been paid to this fact in the experimental literature. The concept of self trapping (extrinsic or intrinsic) is based on the short-range deformation potential due to acoustic phonons [6]. In crystals with the diamond structure it is well known that the sp_3 bond-bending forces are much weaker than the bond-length forces [34]. This is why the short-wavelength TA (or shear-mode) phonons in Si and GaAs have nearly three times less energy than the zone-edge LA (or compression-mode) phonons [25]. One would thus expect broken-bond (or vacancy) type defects to distort most readily in configurations which have the basic symmetry of the zone-edge TA lattice modes. Indeed, this is precisely the distortion symmetry seen by EPR for the silicon vacancy [1]. The importance of zone-edge TA phonons for vacancy defects is further supported by the prediction [35] and observation [36] of negative-U properties for the silicon vacancy. This is a direct consequence of Baraff, Kane, and Schlüter's [35] model of the lattice which is based on Watkin's EPR results [1] and thus specifically adjusted to fit the zone-edge TA phonons rather than the more usual zone-center parameters [34].

The fact that certain defects couple strongly to zone-edge TA modes during nonradiative recombination takes on added significance in view of the very recent phonon transport results of Ulbrich, Narayanamurti, and Chin [37]. These authors find that the zone-edge TA modes in GaAs are "bottlenecked" with respect to decay to lower energy phonons and hence have an exceedingly long mean free path for ballistic transport at He temperatures. The short wavelength TA modes in the diamond structure have an unusually flat dispersion relation [25,34] and hence the group velocity approaches zero at the zone boundary. Thus even at room temperature, MPE recombination along an extended broken-bond type defect (such as a dislocation or vacancy cluster) might be expected to set up a long-lived "standing wave" of zone-edge TA phonons with nearly zero group velocity. Such a concentration of intense short wavelength vibrations set up by multiple-recombination events might be able to move existing defects or create new defects much more effectively than a single recombination event [3]. Indeed, this multiple-recombination TA-mode mechanism could be a very effective new class of recombination-enhanced reactions which might help explain the still mysterious phenomenon of the rapid growth of dislocation networks (dark-line defects) in semiconductor lasers [38].

V. Microscopic Model of DX Centers

Based on the early data for DX centers in Te-doped $Al_xGa_{1-x}As$ and on early theoretical results for unrelaxed vacancies in GaAs, Lang, Logan and Jaros [5] speculated that a likely microscopic model for this defect would be an arsenic-vacancy-plus-donor pair. Such a defect is shown in Fig. (9). A similar self-trapping DX defect was also seen in $Al_xGa_{1-x}As$ doped with other donors (Se, Sn, and Si) [29]. The chemical trends in the optical and trapping properties of these centers could only be explained by different lattice-relaxation force constants in the filled and empty state. This corresponds to different curvatures of the cc diagrams, as shown in Fig. (10). The relative changes in the force constants in Fig. (10) were found to scale remarkably well with the pure Si, GaAs, or Sn force constants corresponding to the atom in Fig. (9) occupying the Ga site next to the arsenic vacancy, namely, Si or Sn for material doped with these donors or Ga (Al) for Te- or Se-doped material [29].

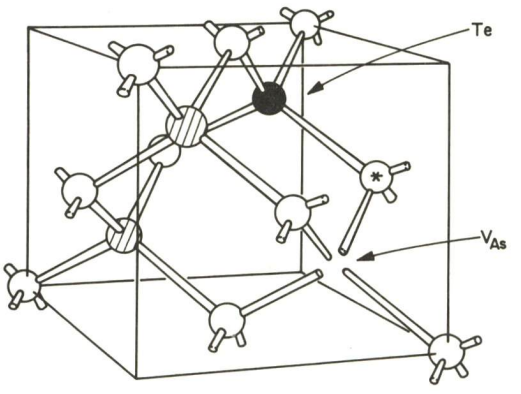

Figure 9. Microscopic model for DX centers. (after Lang et al [5])

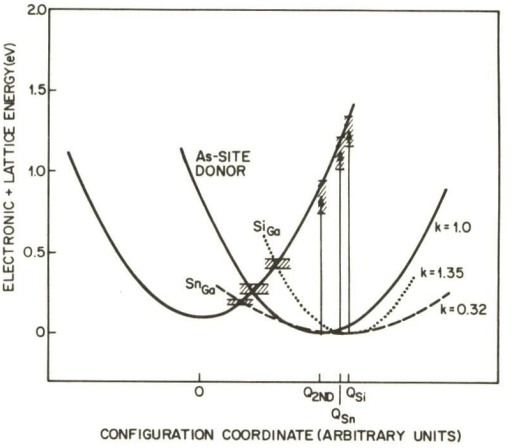

Figure 10. Configuration coordinate diagrams for Te, Se, Sn, and Si DX centers in $Al_xGa_{1-x}As$ (after Lang and Logan [29])

The extreme softness of the occupied Sn-DX center shown in Fig. (10) was explained in terms of a transition between a grey-tin-like (empty) and white-tin-like (filled) structure for the donor-vacancy pair in analogy with the anomalous structure found by Watkins for the tin-vacancy pair in silicon [39]. Watkins [39] also found the vibrational frequency of the tin atom in this pair to be $\hbar\omega = 6$ meV; this is equal to the zone-edge TA phonon energy in grey tin [34]. Since the Te-DX centers also have $\hbar\omega$ equal to the zone-edge TA phonons in GaAs, it is tempting to suggest that the proposed grey-to-white-tin-like behavior in Fig. (10) for Sn-DX centers is related to the structural instability of grey tin against short wavelength shear distortions [34].

The chemical trends in Fig. (10) thus seem to support the model of Fig. (9). Even stronger support comes from the recent phonon absorption results of Narayanamurti et al [40]. This very elegant experiment measured directly the absorption of ballistic acoustic phonons by DX centers in Sn- and Te-doped $Al_xGa_{1-x}As$. By using different propagation directions, these workers were able to determine directly the symmetry of the centers and to show that the centers absorb TA modes much more strongly than LA modes. The results agree exactly with the defect model in Fig. (9). Namely, <111> trigonal symmetry for the Sn-DX center and <110> orthorhombic symmetry for the Te-DX center.

VI. SUMMARY

We have reviewed the evidence for strong electron-phonon coupling at deep level defects in III-V semiconductors. We find that the nonradiative capture rates at many defects are described very well at all temperatures by the semiclassical strong-coupling limit of the multiphonon emission (MPE) theory. The two main parameters controlling the temperature dependence of MPE capture in this limit are the classical barrier height and the phonon energy. We show that capture at most deep levels can be adequately explained by using optical phonon energies but that two defects (DX and EL2), showing anomalous metastable effects at low (<77K) temperatures, can only be fit with the much softer zone-edge transverse acoustic (TA) modes. We discuss how one theoretically expects extrinsic self-trapping and vacancy-like defects to be strongly coupled to such short-wavelength TA modes and propose a mechanism whereby the vanishing group velocity and long life of these TA modes might be an essential key to understanding multiple-recombination enhanced reactions in these materials. Finally, we discuss the microscopic model for the extrinsic self-trapping DX centers in $Al_xGa_{1-x}As$ and show how recent evidence strongly supports the original donor-plus-arsenic-vacancy model proposed for this class of centers.

References

1) G. D. Watkins: proceedings of the Int'l Conf. on Crystal Defects, Conf. J. Phys. Soc. Jpn. 18 (1963) 22.

2) H. Kukimoto, C. H. Henry and F. R. Merritt: Phys. Rev. B7 (1973) 2486.

3) D. V. Lang and L. C. Kimerling: Phys. Rev. Lett. 33 (1974) 489.

4) C. H. Henry and D. V. Lang: Phys. Rev. B15 (1977) 989.

5) D. V. Lang, R. A. Logan and M. Jaros: Phys. Rev. B19 (1979) 1015.

6) Y. Toyozawa: Solid State Electronics. 21 (1978) 1313.

7) R. Englman and J. Jortner: Mol. Phys. 18 (1970) 145.

8) K. Huang and A. Rhys: Proc. Roy. Soc. 204 (1950) 406.

9) R. Kubo and Y. Toyozawa: Prog. Theor. Phys. 13 (1955) 160.

10) M. Lax: J. Chem. Phys 20 (1952) 1752.

11) C. H. Henry: In *Relaxation of Elementary Excitations*, eds. R.Kubo and E. Hanamura (Springer-Verlag, Berlin, 1980), p. 19.

12) N. F. Mott: Proc. Roy. Soc. London A167 (1938) 384.

13) N. F. Mott: Solid-State Electronics. 21 (1978) 1275.

14) C. W. Struck and W. H. Fonger: J. Lum. 10 (1975) 1.

15) D. J. Robbins and A. J. Thomson: Phil. Mag. 36 (1977) 999.

16) D. V. Lang and R. A. Logan: J. Electronic Mat. 4 (1975) 1053.

17) D. V. Lang and C. H. Henry: Phys. Rev. Lett. 35 (1975) 1525.

18) B. K. Ridley: J. Phys. C. 11 (1978) 2323.

19) R. Pässler: Phys. Stat. Sol. (b) 86 (1978) K39.

20) M. G. Burt: J. Phys. C. 13 (1980) 1825.

21) As has been pointed out in ref. 19, there is a slight discrepancy between the level B data in refs. 4 and 17 as compared with that in ref. 16 due to the values of v_{th} used. Reference 16 and the current Fig. 2 are the most accurate.

22) See eg. H. C. Casey, Jr. and M. B. Panish, *Heterostructure Lasers* (Academic Press, New York, 1978) p. 120.

23) H. G. Grimmeiss: Ann. Rev. Mater. Sci. 7 (1977) 341.

24) G. M. Martin, A. Mitonneau, and A. Mircea: Electronics Letters 13 (1977) 191.

25) G. Dolling and R. A. Cowley: Proc. Phys. Soc. 88 (1966) 463.

26) E. P. Sinyavskii and V. A. Kovarskii: Fiz. Tverd. Tela 9 (1966) 1464. [Sov. Phys. - Solid State 9 (1967) 1142].

27) D. V. Lang and R. A. Logan: Phys. Rev. Lett. 39 (1977) 635.

28) R. J. Nelson: Appl. Phys. Lett. 31 (1977) 351.

29) D. V. Lang and R. A. Logan: Proc. 14th Int'l Conf. on the Physics of Semiconductors, Edinburg., 1978. (Inst. Phys. Conf. Ser. No. 43, 1979) p.433.

30) R. A. Craven and D. Finn: J. Appl. Phys. 50 (1979) 6334.

31) Y. Toyozawa: In *Relaxation of Elementary Excitations*, eds. R. Kubo and E. Hanamura (Springer-Verlag, Berlin, 1980), p. 3.

32) D. Emin: Adv. Phys. 22 (1973) 57.

33) The data of Nelson (ref. 28) has been shifted from his arbitrary definition of the rate constant to a value consistent with the definition used in ref. 27, namely, the average of the log of the rate distribution for a highly nonexponential transient.

34) J. C. Phillips: *Bands and Bonds in Semiconductors*, (Academic Press, New York, 1973).

35) G. A. Baraff, E. O. Kane, and M. Schlüter: Phys. Rev. Lett. 43 (1979) 956.

36) G. D. Watkins and J. R. Troxell: Phys. Rev. Lett 4 (1980) 593.

37) R. G. Ulbrich, V. Narayanamurti, and M. A. Chin: Phys. Rev. Lett. (to be published) and Proc. of this Conference.

38) For references see I. Hayashi: Proc. of this Conf.

39) G. D. Watkins: Phys. Rev. B12 (1975) 4383.

40) V. Narayanamurti, R. A. Logan, and M. A. Chin: Phys. Rev. Lett 43 (1979) 1536.